# The retinoic acid receptor drives neuroinflammation and fine tunes the homeostasis of interleukin-17-producing T cells

Rasmus Agerholm[1], John Rizk[1], Darshana Kadekar[1], Annie Borch, Sine Reker Hadrup, and Vasileios Bekiaris*[1]

**Affiliations:**

[1]Department of Health Technology, Technical University of Denmark, Kemitorvet, Bldg 202, 2800 Kgs Lyngby, Denmark.

*Address correspondence to Vasileios Bekiaris vasbek@dtu.dk

**One sentence summary:** Retinoic acid receptor activity was required on IL-17-producing $CD4^+$ and γδ T cells to induce their neuropathogenicity, and to regulate both positively and negatively their homeostasis.

## Abstract

The vitamin A metabolite retinoic acid (RA) and its receptor (RAR) are one of the key interactions regulating cellular immunity and neural signaling. Whether endogenous RA-RAR interactions contribute to the development of neuroinflammation and diseases like multiple sclerosis, remains to be elucidated. Herein, we used the murine experimental autoimmune encephalomyelitis (EAE) model and an established genetic RAR silencing approach to decipher its role in pathogenic T cell responses. We show that RAR is necessary for the development of interleukin(IL)-17-driven, cell-mediated immunopathology in the brain and that it fine tunes the homeostasis of IL-17-producing gamma delta (γδT17) and $CD4^+$ T cells ($T_H17$). At steady-state, RAR was required in the γδT17 compartment to sustain optimal cell numbers and maintain expression of genes involved in cell cycle progression. In contrast, RAR negatively regulated T helper-17 ($T_H17$) cell homeostasis. Our data show that RAR is required during the early phases of EAE in order to induce a γδT17 response and that its activity is necessary throughout the course of the disease to allow $T_H17$ and γδT17 cells to infiltrate the brain. This is correlated with failure of RAR deficient cells to express surface integrin-alpha4, a major brain homing molecule. Collectively, our work demonstrates that endogenous RA-RAR interactions are important for the homeostasis of IL-17-producing T cells and necessary for their pathogenicity during neuroinflammation.

## Introduction

Retinoic acid (RA) is an active metabolite of vitamin A that regulates a large number of cellular processes (*1*). The effects of RA are mediated through its transport to the nucleus and binding to RA receptor (RAR)-retinoid X receptor (RXR) dimers, which initiate gene transcription (*2, 3*). RAR-RXR dimers are ubiquitously expressed and active, hence explaining the pleiotropic role of RA ranging from neuronal development to bone morphology (*4-6*). In the immune system the RA-RAR interaction promotes formation of secondary lymphoid tissues (*7, 8*) during embryogenesis, while in adulthood, RA production by dendritic cells induces expression of the gut homing molecules CCR9 and α4β7 on T cells and innate lymphoid cells (*9-11*). Besides imprinting gut-tropism, RA is critical for the differentiation of T-helper ($T_H$) cells and the balance between $T_H$ cell subsets. Thus, vitamin A insufficient mice fail to generate $T_H1$ and $T_H17$ responses in the intestine after infection (*12*), whereas microbiota-driven $T_H17$ differentiation is impaired (*13*). Generation of regulatory T ($T_{REG}$) cells post immunization also appears to be RA dependent (*12*), which agrees with the requirement of RA for *in vitro* $T_{REG}$ differentiation (*14-16*). Furthermore, RA regulates $T_H17$ to $T_H1$ plasticity (*17*) and is critical for the development of small intestinal intra-epithelial lymphocytes (*18, 19*).

$T_H17$ cells together with IL-17-producing gamma delta T (γδT17) cells are the major pathogenic populations in animal models of neuroinflammation, such as experimental autoimmune encephalomyelitis (EAE) (*20-22*), and their presence correlates with disease severity in human multiple sclerosis (MS) (*23-26*). Hence, suppressing IL-17-secreting T cells is a goal in a number of treatments aiming to reduce MS pathology (*27-29*). In this regard, it has been shown that administration of RA during ongoing EAE or pre-treatment of donor cells with RA prior to transfer into recipient mice can suppress the function of both $T_H17$ and γδT17 cells and impair their pro-inflammatory capacity (*30, 31*). In addition to inhibiting T cell responses, administration of RA can reduce the production of cytokines by microglia and astrocytes (*32*). Similarly, astrocytes have been shown to be a source of RA, which under inflammatory conditions protects the blood-brain barrier (*33*). These experiments indicate that exogenously administering RA will have a clear systemic impact on multiple cellular and tissue compartments making it difficult to assess its

precise mechanism of action and its therapeutic potential in MS. It is therefore not surprising that clinical trials with dietary vitamin A supplementation or synthetic RA compounds have yielded mixed results (*34*).

Although most of our knowledge regarding the role of RA and RAR in neuroinflammation stems from in vivo and in vitro treatments with RA itself or retinoid-related compounds, there is no evidence regarding the importance of endogenous RA. Herein, we used a genetic mouse model whereby RAR is rendered inactive in cells producing IL-17 and showed that active RAR is necessary for $T_H17$ and γδT17 cells to respond to neuroinflammatory stimuli, infiltrate the brain and cause pathology. Thus, mice with inactive RAR in $T_H17$ and γδT17 cells are resistant to EAE and display limited T cell infiltration in the brain. We additionally provide evidence that RAR is important to maintain a normal homeostatic environment for IL-17-producing T cells. Our data demonstrate the importance of endogenous RA-RAR interactions in driving neuropathogenic T cell responses and emphasize the need for re-evaluating our efforts in using vitamin A and RA supplementation as a treatment for MS.

## Results

### Reduced RAR activity in γδT17 and $CD4^+$ T cells derived from $ROR\gamma t^{CRE}$-$RARdn^{F/F}$ mice

In order to test the importance of RAR inactivation in IL-17-producing T cells we used mice where expression of the Cre recombinase is driven by the promoter of the transcription factor RORγt, which is highly expressed in IL-17-producing lymphocytes. We crossed $ROR\gamma t^{CRE}$ mice (*35*) with mice whereby constitutive expression of a RAR dominant negative (dn) transgene within the *ROSA26* locus was prevented by a floxed stop codon ($RARdn^{F/F}$) (*36*). Excision of the stop codon allows constitutive RARdn transgene expression, which prevents endogenous RAR from becoming activated (*36*). Using $ROR\gamma t^{CRE}$-$RARdn^{F/F}$ mice, we recently showed that in the gut, RAR is important for the production of IFN-γ by $Tbet^+$ γδT17 cells (*20*). Owing to their importance in brain inflammation in EAE, we focused our current investigation on $CD4^+$ of the $T_H17$ lineage and γδT17 cells.

In lymphoid tissues like lymph nodes (LNs), γδT17 populations can be phenotypically identified by flow cytometry as $CD27^{-}CD44^{+}CCR6^{+}$, and can express either the Vγ4 or the Vγ6 ($Vγ4^{-}$) TCR chains (*37, 38*) (Vγ nomenclature according to Heilig & Tonegawa (*39*)). Because the $Vγ4^{+}$ population has been shown to be more pathogenic during neuroinflammation (*40*), we analyzed separately Vγ4- and Vγ6-expressing cells. To confirm that the RARdn transgene was expressed, we FACS-sorted $Vγ4^{+}$ or $Vγ4^{-}$ γδT17 cells from the LN of $RORγt^{CRE}$-$RARdn^{F/F}$ mice, and compared them to γδT17 cells derived from littermate control mice, or to $CD27^{+}$ γδ T cells, which are $RORγt^{-}$ and do not produce IL-17 (*38*). Only $Cre^{+}$ γδT17 cells expressed the transgene (Fig. S1a). Because RORγt is transiently expressed in double-positive thymocytes, we assessed RARdn expression in $CD4^{+}$ T cells, and found it present, albeit at lower levels than in γδT17 cells (Fig. S1a). This was most likely due to the reduced activity of the RORγt-driven Cre recombinase in $CD4^{+}$ T cells, as we have shown before (*41*).

In order to test whether the transgene was active in the aforementioned populations, we assessed surface expression of the gut homing receptors CCR9 and α4β7, both of which require RA-RAR interactions to be induced (*9*). Being an inductive site for gut homing lymphocytes, mesenteric LN (mLN) derived γδ T cells had higher levels of surface CCR9 and α4β7 compared to cells from the peripheral skin draining LNs (pLNs) (Fig. S1b). Both molecules displayed lower abundance in cells from $RORγt^{CRE}$-$RARdn^{F/F}$ mice (Fig. S1c), however α4β7 levels were very low in the pLNs and there was no detectable difference between transgenic and littermate control mice (Fig. S1c). Similar to mLNs, surface CCR9 was reduced in γδT17 cells derived from the small intestinal or colonic lamina propria (Fig. S1d). We could not detect α4β7 in gut γδT17 cells. Although expression of the RARdn transgene was low in $CD4^{+}$ T cells (Fig. S1a), we found that in cells derived from transgenic mice, surface abundance of CCR9 and α4β7 was reduced (Fig. S2a), indicating that despite its low levels, the transgene was active in this cellular compartment. It is noteworthy, that CCR9 and α4β7 could only be detected in $CD4^{+}$ T cells expressing CD44 (Fig. S2b, c), an adhesion molecule most often used as a memory marker on mouse T cells. This data suggests that in our model, there is loss of RAR activity in γδT17 and activated $CD4^{+}$ T cells.

**RAR is required for normal γδT17 cell homeostasis**

In order to begin addressing the in vivo importance of RAR in γδT17 cells, we enumerated LN $CD27^{-}CD44^{+}CCR6^{+}$ cells and found that their frequency was reduced in $ROR\gamma t^{CRE}$-$RARdn^{F/F}$ mice compared to littermate controls (Fig. 1a) with no apparent deficit in their numbers (Fig. 1b). In these mice the frequency of $V\gamma4^{+}$ γδT17 cells was significantly decreased whereas that of $V\gamma4^{-}$ cells was concomitantly increased (Fig. 1c, d). When we analyzed their numbers, we found a small but significant decrease in $V\gamma4^{+}$ cells (Fig. 1e), whereas $V\gamma4^{-}$ cells remained unchanged (Fig. 1e).

Intracellular staining for IL-17A recapitulated the above findings. Thus, $ROR\gamma t^{CRE}$-$RARdn^{F/F}$ mice contained significantly reduced IL-17A-producing $V\gamma4^{+}$ but not $V\gamma4^{-}$ γδ T cells (Fig. 2a), and as a result the frequency of $IL\text{-}17A^{+}V\gamma4^{+}$ cells was lower than the frequency of $IL\text{-}17A^{+}V\gamma4^{-}$ cells (Fig. 2b, c). To test whether the ability of the cells to produce IL-17A was also compromised, we measured its mean fluorescent intensity (MFI) and found no difference (Fig. 2d). In order to assess production of IL-22 we stimulated bulk LN cells with IL-23. We found that similar to what we observed with IL-17A, the frequency of $IL\text{-}22^{+}V\gamma4^{+}$ cells was lower, while that of $IL\text{-}22^{+}V\gamma4^{-}$ cells was higher in $ROR\gamma t^{CRE}$-$RARdn^{F/F}$ mice compared to littermate controls (Fig. 2e, f). Inactive RAR did not affect IL-22 secretion (Fig. 2g). Collectively, our data show that in the LN, RAR is required to maintain normal γδT17 cell homeostasis by specifically regulating numbers of the Vγ4-expressing population.

**RAR regulates transcription of cell cycle genes in $V\gamma4^{+}$ γδT17 cells**

Due to their specific involvement in driving inflammatory diseases including neuropathogenesis in the context of EAE (*40, 42*), we aimed at elucidating the mechanism by which RAR regulates the Vγ4-expressing γδT17 population. We found that RAR did not impact on the expression of IL-7R and RORγt (Fig. S3a), both of which are important in regulating the homeostasis and proliferation of γδT17 cells (*43-46*). We then reasoned that decreased $V\gamma4^{+}$ cell numbers were due to defective embryonic thymic development. However, newborn $ROR\gamma t^{CRE}$-$RARdn^{F/F}$ thymi contained normal numbers of $V\gamma4^{+}$ γδT17 cells and slightly but significantly elevated $V\gamma4^{-}$ cell numbers (Fig. S3b), suggestive of a post-embryonic defect.

To further characterize the molecular changes that occur in γδT17 cells in the absence of active RAR, we performed RNA-sequencing (RNA-seq) from FACS-sorted $CD27^{-}CD44^{+}V\gamma4^{+}$ and

144 CD27$^{-}$CD44$^{+}$Vγ4$^{-}$ γδ T cells derived from LNs of adult RORγt$^{CRE}$-RARdn$^{F/F}$ and littermate control
145 mice. Principal component analysis (PCA) showed that RAR inhibition did not have a significant
146 effect on global gene expression (Fig. S4a). Assessment of Vγ and Vδ chain genes confirmed the
147 homogeneity of the sorted Vγ4$^{+}$ population and showed that Vγ4$^{-}$ cells expressed Vγ6 (Fig. S4b).
148 Next, we examined whether there were differentially expressed genes between Cre$^{+}$ and Cre$^{-}$
149 cells and found that within the Vγ4$^{+}$ population, RAR-deficiency correlated with significantly
150 reduced expression of 71 genes and induced expression of 39 (Fig. 3a and Fig. S4c). Within the
151 Vγ4$^{-}$ population there were 26 genes down- and 19 genes up-regulated significantly (Fig. 3a and
152 Fig. S4d). Most of the gene expression profiles affected by RAR did not overlap between Vγ4$^{+}$ and
153 Vγ4$^{-}$ γδ T cells (Fig. 3a), suggesting subset-specific regulation. In order to understand the
154 biological processes that these gene changes were affecting we performed pathway analysis of
155 the differentially expressed genes in RORγt$^{CRE}$-RARdn$^{F/F}$ Vγ4$^{+}$ cells using GOrilla (*47, 48*). The
156 differentially expressed genes in Vγ4$^{-}$ cells and the up-regulated ones in the Vγ4$^{+}$ cells did not
157 enrich for any pathway. However, the genes that were down-regulated in the absence of RAR
158 activity in Vγ4$^{+}$ cells were enriched in processes associated with cell cycle and division, mitosis
159 and chromosomal segregation (Fig 3b). Such genes included cyclins (e.g. *Cdc25c*, *Ccnb1*, *Cdc6*),
160 kinetochore-associated (e.g. *Zwilch*, *Ska1*, *Ska3*, *Nsl1*) or centrosome-associated (e.g. *Fignl1*,
161 *Poc1a*) genes.
162 This data indicated that RAR may regulate homeostatic turnover of Vγ4$^{+}$ γδT17 cells. To
163 directly assess this, we examined expression of the cell cycle progression marker Ki67 at steady-
164 state. However, there was not a difference in the percentage of cycling cells within the Vγ4$^{+}$
165 population (Fig. 3c). Collectively, our data demonstrate that although RAR is required for the
166 transcription of a number of genes required for cell cycle progression, this does not manifest as a
167 defect in G-S phase transition at homeostatic conditions.
168
169 **RAR negatively regulates $T_H$17 cell homeostasis**
170 Since we discovered that the RARdn transgene was active in CD4$^{+}$ T cells (Fig. S2), it was
171 important to assess their homeostasis in RORγt$^{CRE}$-RARdn$^{F/F}$ mice. In this regard, in the pLN or
172 mLN, lack of active RAR resulted in equal numbers of total CD4$^{+}$ but significantly higher

$CD4^+CD44^+$ T cells (Fig. 4a and Fig. S5a). Because expression of the transgene is driven by RORγt, we sought to more closely investigate $T_H17$ cells, which at steady-state express the chemokine receptor CCR6 (*49, 50*). To confirm that $CD4^+CCR6^+$ T cells were $T_H17$-enriched, we analyzed mice expressing GFP (green fluorescent proteins) under the control of the RORγt promoter and AmCyan under the control of the Tbet promoter (*20*). We show that the $CD4^+CCR6^+$ population contains very few Tbet-expressing cells and approximately 80% of them are $ROR\gamma t^+$ (Fig. 4b). Moreover, all of the CCR6-expressing cells were $CD44^+$ (Fig. 4c). Next, we assessed numbers of $CD4^+CCR6^+$ T cells, and found that they were significantly increased in the LNs of $ROR\gamma t^{CRE}$-$RARdn^{F/F}$ mice compared to controls (Fig. 4d and Fig. S5b). In contrast, numbers of $CD4^+CCR6^-$ cells, were not affected in $ROR\gamma t^{CRE}$-$RARdn^{F/F}$ mice (Fig. 4d), suggesting that the major impact of RAR in these animals is on $T_H17$ cells. In agreement with this, we detected significantly more IL-17- and IL-22-producing $CD4^+CD44^+$ T cells in LNs of mice with inactive RAR (Fig. 4e). Since, the intestine is enriched in $T_H17$ cells, we additionally analyzed small intestinal lamina propria lymphocytes and found significantly elevated frequencies of IL-17-producing $CD4^+$ T cells (Fig. S5c). Collectively, our data suggests that RAR negatively regulates the numbers and IL-17 production of $T_H17$ cells at steady-state.

**$ROR\gamma t^{CRE}$-$RARdn^{F/F}$ mice are resistant to EAE**

A combined response between $T_H17$ and γδT17 cells is required for the development and progression of experimental autoimmune encephalomyelitis (EAE) (*21, 22*). We therefore induced EAE in $ROR\gamma t^{CRE}$-$RARdn^{F/F}$ and littermate control mice and assessed disease progression as well as T cell responses in the LNs, spleen, and brain at the peak of the disease. We found that by comparison to controls, $ROR\gamma t^{CRE}$-$RARdn^{F/F}$ mice were resistant to EAE symptoms (Fig. 5a) and showed reduced weight loss (Fig. 5b). Paralysis in EAE is caused by infiltration of pathogenic T cells in the brain. We found that contrary to control symptomatic animals, mice with defective RAR had very few $CD4^+CD44^+$ and γδT17 cells in the brain at the peak of the disease, 21 days post-immunization (Fig. 5c, d). Of note, expression of CCR6 was almost undetectable in the brain (Fig. 5c), most likely reflecting the local production of CCL20 by choroid plexus epithelia (*51*). When we analyzed the CD4 responses in the LNs and spleen we found elevated numbers of $CD4^+CD44^+$ T

cells, irrespective of whether they were $CCR6^+$ or $CCR6^-$ (Fig. S6a, b). Numbers of γδT17 cells were not changed at that time point (Fig. S7a, b). We additionally tested the capacity of both $CD4^+$ and γδ T cells to produce IL-17. We found that although there was no difference in the frequency of IL-17-producing $CD4^+$ T cells at day 21, production of IL-17 did not increase between unimmunized and immunized $ROR\gamma t^{CRE}$-$RARdn^{F/F}$ mice (Fig. 5e and Fig. S6c). Production of IL-17 by γδ T cells was slightly but significantly decreased in LNs and spleen at day 21 (Fig. 5f and Fig. S7c). Therefore, effective RA-RAR interactions are necessary for T cells to infiltrate the brain and cause neuropathology, but have a minor impact on lymphoid tissue responses at the peak of the disease.

**RAR is important to initiate γδT17 responses and sustain integrin-α4 during EAE**

Next, we wanted to investigate why there was a failure to infiltrate the brain and why RAR deficiency had such a profound impact on disease progression. It has been shown recently that early events driven primarily by γδ T cells are critical to establish disease progression in EAE (*40*). We therefore assessed both γδ and $CD4^+$ T cell responses in $ROR\gamma t^{CRE}$-$RARdn^{F/F}$ and littermate control mice, at day 11, before any clinical symptoms were observable. As expected, the $CD4^+$ T cell response was not compromised in transgenic animals, instead there was a consistent increase in the numbers of $CD4^+CCR6^+$ T cells (Fig. 6a, b). In contrast, there was a profound reduction in γδT17 cell numbers in the spleen and LNs (Fig. 7a, b). This difference could be attributed to a failure of the Vγ4-expressing population to expand in response to immunization (Fig. 7a, b). Thus, during the early phases of the disease, RAR is critical to initiate γδT17-driven inflammation, especially of the $V\gamma4^+$ population.

As we showed earlier (Fig. S1) and others before, RAR is critical for the expression of the gut homing receptor α4β7. In addition to pairing with the β7 chain, the α4 integrin (CD49d) can also pair with the β1 chain to form the α4β1 integrin (VLA-4), which is important for entry of pathogenic lymphocytes into the brain during EAE (*52, 53*). Furthermore, blockade of α4 with a humanized monoclonal antibody (natalizumab), has been licensed as a therapeutic intervention for MS (*54*). We therefore assessed the levels of expression of integrin-α4 (Itgα4) during EAE in $CD4^+$ and γδ T cells from $ROR\gamma t^{CRE}$-$RARdn^{F/F}$ and littermate control mice. We found that RAR deficient $CD4^+$ T

cells expressed significantly lower amounts of Itgα4 at day 11 following MOG immunization (Fig. 6c-e). In γδT17 cells, there was reduced expression of Itgα4 in the Vγ4$^{+}$ but not the Vγ4$^{-}$ population (Fig. 7d, e). Collectively, this data suggests that during neuroinflammation, in addition to initiating γδT17 expansion, RAR sustains expression of Itgα4 in both the CD4$^{+}$ and γδ T cell compartments, which might explain why effector IL-17-producing cells do not infiltrate the brain and cause pathology in RORγt$^{CRE}$-RARdn$^{F/F}$ mice.

## Discussion

In the present study we provide evidence that RA-RAR interactions are necessary to induce IL-17-driven brain pathology. Active RAR was required by the Vγ4-expressing subset of IL-17-producing γδ T cells in order to mount an early encephalitogenic response, and by IL-17-producing CD4$^{+}$ and γδ T cells to infiltrate the brain; most likely due to reduced levels of surface Itgα4. Furthermore, we provide evidence that RAR is a negative regulator of $T_H17$ homeostasis, whereas it positively regulates the homeostasis of γδT17 cells. Hence, inactivation of RAR led to a subset-specific suppression of γδT17 cells and correlated with reduced expression of cell cycle genes, whereas it increased the numbers of $T_H17$ cells at steady-state.

Sensing of intracellular RA by RAR initiates cell subset transcriptional programs that are as diverse as phototransduction and organogenesis (*6*). In the central nervous system, RA plays an indispensable role during development, while it also appears to be important in regulating the homeostatic function of the adult brain (*55*). Simultaneously, unperturbed RA-RAR interactions are necessary for the normal function of most immune cells (*1*). It has therefore been very hard to pinpoint the precise biological importance of RA and RAR in neuroinflammatory diseases such as MS. Our data shows that active RAR is necessary in IL-17-producing T cells to become activated in response to neuroinflammatory signals, infiltrate the brain and cause disease. These findings agree with the notion that RA-RAR interactions are critical for a functional immune system, including when the response is pathogenic. Therefore, acute ablation of the RA-RAR interaction may prevent T cell activation or recruitment to the brain and alleviate MS-associated symptoms.

Given that the vast majority of the western population, including MS patients, do not suffer from vitamin A deficiency, it is endogenous, homeostatic levels of RA that fine tune both immune

and neurological function. Therefore, dietary supplementation for the treatment of MS may be unnecessary or redundant, which might explain why related clinical trials have yielded mixed results (*34*). Synthetic RA or RA-related compounds have been shown before to have direct and acute influence on the immune system (*12*). In this regard, an exogenously supplied RA mimic in mice delayed induction of EAE (*30*). Whether the compound acted on the immune system or directly in the brain was not addressed, while the apparent inhibition on IL-17 by $CD4^+$ T cells was only evident after continuous in vitro stimulation (*30*). Similarly, in vitro treatment of T cells with RA prior to adoptive transfer in recipient animals under conditions inducing EAE, suppressed IL-17 and lowered disease incidence (*31*). However, the in vivo immuno-modulatory effects of RA administration on IL-17-secreting populations during EAE have not been elucidated. Although our findings argue that RA is necessary for the optimal activation of IL-17-producing T cells during inflammation, it is plausible that exogenous RA may act indirectly or as a death-inducing molecule (*56*) to promote immuno-suppression.

One of the most well-studied effects of RA on immune cells, especially T cells, is tissue homing through regulation of the chemokine receptor CCR9 and the integrin subunit Itgα4 (*9*), both of which are RA inducible genes (*57, 58*). The α4 subunit can pair with Itgβ1 to form the brain-homing integrin α4β1, also known as VLA-4 (*52, 53*). The importance of Itgα4 in regulating the homing of pathogenic immune cells to the brain is exemplified by the use of an anti-Itgα4 blocking antibody for the treatment of MS patients (*54*). In our studies, diminished infiltration of pathogenic T cells in the brain when RAR was inactive, correlated with very low levels of Itgα4. This suggests that during conditions of neuroinflammation, RA-RAR interactions are necessary to maintain expression of Itgα4 and allow T cells to home to the brain. Therefore, therapeutic targeting of the RA pathway is very likely to alter the migratory capacity of encephalitogenic T cells.

In addition to adhesion and migration, RA regulates a plethora of immunological processes, which are often cell subset and context dependent. In this regard, lack of active RAR affected only the Vγ4-expressing subset of γδT17 cells both at steady-state and during the early stages of neuroinflammation. This was somewhat unexpected since recent RNA-seq analyses indicated that in the LNs, the two γδT17 subsets ($Vγ4^+$ and $Vγ6^+$) are nearly identical (*59*). It is plausible that the two subsets occupy distinct niches within the LN where RA may be differentially produced by

accessory cells within the immediate microenvironment. A potential underlying mechanism by which RA regulates γδT17 subsets is by fine tuning the expression of cell cycle genes, a process that is well-documented in different cell types (*4, 56*). Thus, intact RA production and RAR activity are important for optimal proliferation of fetal cardiomyocytes (*60*), endothelial vasculature (*61*), intestinal stem cells (*62*) and cerebral glial cells (*36*). However, there is limited information on whether and how RA and RAR regulate T cell proliferation. It has been shown that RA can boost in vitro human T cell proliferation by regulating cyclin D proteins (*63, 64*), while in vivo, RAR enhanced $CD4^+$ T cell proliferation during intestinal infection with the parasite *Toxoplasma gondii* (*12*). Our data clearly show that at steady-state RAR negatively regulates the number of $T_H17$ cells, a defect that was evident throughout the course of EAE.

Collectively, our data show that intrinsic RA-RAR interactions are necessary for the development of pathogenic neuroinflammation by establishing a coordinated response by IL-17-producing T cell subsets and promoting their ability to infiltrate the brain. Furthermore, we provide evidence that RAR is a critical homeostatic rheostat of IL-17-producing T cells by imposing cell subset specific positive and negative regulation. This study highlights the importance of RA and its receptor as key molecular determinants of T cell driven inflammation of the CNS and paves the way for reevaluating their role as potential therapeutic targets in MS.

## Materials and Methods

### Mice

All animal breeding and experiments were performed in house and only after approval from the Danish Animal Experiments Inspectorate. $ROR\gamma t^{CRE}$ (*65*) mice were provided by Gerard Eberl. $RARdn^{F/F}$ mice (*36*) were provided by William Agace after permission from San Sockanathan. $ROR\gamma t^{GFP}Tbet^{AmCyan}$ mice were described before (*20*).

### Cell preparation and culture

Dissected LNs and spleens were isolated and processed as previously described (*41*). Briefly, they were crushed through a cell strainer and washed before being re-suspended in culture media (RPMI containing 10% FBS, Penicillin/Streptomycin, 0.1% β-ME, 20mM HEPES and L-Glutamine)

(media and supplements from ThermoFisher) at the desired density of $10^7$/ml of which $2.5x10^6$ were used for subsequent flow cytometry experiments. An extra RBC lysis step was used for spleens. For cytokine detection $10^7$ cells per well in a 12-well plate were cultured for 3.5 hours in the presence of 50ng/ml PMA, 750ng/ml Ionomycin and $10^{-3}$ diluted Golgi Stop™ (monensin). To detect IL-22 cells were cultured overnight with 40ng/ml recombinant mouse IL-23 (R&D Systems). To prepare γδ T cells and $CD4^+$ T cells for cell sorting, lymphocytes were enriched by magnetic depletion of CD8 T cells and B cells; briefly, $1x10^8$ lymphocytes were re-suspended in MACS buffer (2% FBS, 1 mM EDTA in PBS) and incubated with biotin conjugated anti-CD8 (53-6.7) and anti-CD19 (6D5) at a dilution of 1:200 (both from Biolegend) and 50µL/mL normal rat serum for 10 min at RT. Subsequently, 75µL/mL of BD IMag Streptavidin Particles Plus – DM were added to the mixture and incubated for an additional 2.5 minutes. The samples were incubated for 2.5 minutes in an EasySep™ Magnet and the negative fraction collected.

To prepare lamina propria lymphocytes from the small intestine and colon the tissue was initially flushed with HBSS/HEPES (pH 7.4) and then fat and Peyer's patches were mechanically removed. Tissue was cut into 2-3 cm pieces and washed 4 times (15 min each) in HBSS/2mM EDTA at 37°C shaking followed by digestion with 0.06mg/ml Roche Liberase TM and 0.03mg/ml DNase I (all enzymes from Sigma-Aldrich) for 40 min at 37°C with stirring at 700 rpm. Cell suspension was then pelleted and then re-suspended in 4 mL 40% Percoll (GE Healthcare), layered on 4 mL 70% Percoll and centrifuged at 800x*g (RT)* for 20 min with breaks set to zero. Interphase cells were washed with culture media before further use.

**Experimental Autoimmune Encephalomyelitis**

EAE was induced by sub-cutaneous injection of 50µg of MOG35-55 peptide in CFA, while 200 ng pertussis toxin were intra-peritoneally (i.p.) injected on the day of immunization and 2 days later. From day 11 after immunization and until day 21, mice were weighed and scored for clinical signs as follows: 0: no symptoms; 1: tail paralysis; 1.5: impaired righting reflex; 2: paralysis of one hind limb; 2.5: paralysis of both hind limbs; 3: paralysis of one fore limb; 3.5: paralysis of one fore limb and weak second for limb; 4: total limb paralysis. Mice were euthanized at days 21 after immunization and were perfused with PBS. LN cells were isolated as described above. Brain

tissue was mechanically minced and passed through a 70µm cell strainer to obtain a single cell suspension. Lymphocytes were separated using density gradient centrifugation with 47% Percoll (GE Healthcare), layered on 4 mL of 70% Percoll, and centrifuged at 20 °C and 900 × *g* for 30 min with deceleration set to 0.

**Flow Cytometry**

Cells were stained in U-bottom 96-well plates in 75µl PBS containing 3% FBS with combinations of the following antibodies: CD4-FITC (RM4-4), CD19-FITC (6D5), CD8-FITC (53-6.7), TCRβ-APCeF780 (H57-597; eBioscience), TCRγδ-BV421 (GL3), CD44-V500 (IM7), CCR6-AF647 (140706), Vγ4-PerCPeF710 (UC3-10A6), CCR9-PE (eBioCW-1.2; eBioscience), α4β7-PECF594 (DATK32), CD3-PECy7 (145-2C11), CD27-PECy7 (LG.3A10), Vγ5-FITC (536), CD3-PE (145-2C11; BioLegend), CD3-PECF594 (145-2C11), CCR9-APC (eBIOCW-1.2; eBioscience), CD49d-PE (R1-2; eBioscience), CD69-PECF594 (H1.2F3), CD45-V500 (30-F11), RORγt-APC (B2D), CD127-BUV737 (SB/199), IL-17A-BV786 (TC11-18H10), IL-22-PE (1H8PWSR; eBioscience), IFNγ-PE (XMG1.2; BioLegend), IFNγ-APC (XMG1.2; BioLegend), Ki67-BV786 (B56). Cells were stained for 30 minutes on ice and all antibodies were used at a 1:200 dilution, expect Ki67 which was used at a 1:100 dilution. Prior to antibody staining cells were incubated with 100ul PBS containing $10^{-3}$ diluted Fixable Viability Dye AF700 for 10 minutes on ice. Cells were washed in 150µl PBS containing 3% FBS in-between steps. Intracellular cytokine staining was performed using the BD Cytofix/Cytoperm Kit™ according to the manufacturer's instructions. Transcription factor staining was performed using the eBioscience FoxP3 Transcription Factor Staining kit according to the manufacturer's instructions. Unless specified all antibodies and staining reagents were purchased from BD Biosciences. Samples were acquired on a BD LSR Fortessa™ using BD FACSDiva software v8.0.2.

**Bulk RNA-seq**

Lymphocytes were isolated from peripheral, cervical and auricular LNs of RORγt$^{CRE}$-RARdn$^{F/F}$ or littermate control mice and γδ T cells were enriched as described above. Subsequently, Vγ4$^{+}$TCRγδ$^{+}$CD3$^{+}$CD44$^{+}$CD27$^{-}$ and Vγ4$^{-}$TCRγδ$^{+}$CD3$^{+}$CD44$^{+}$CD27$^{-}$ populations from each mouse

strain were sorted using a FACSAriaIII: populations into RNA protect (QIAGEN, Hilden, Germany). Total RNA was extracted from the sorted cells according to the “Purification of total RNA from animal and human cells” protocol of the RNeasy Plus Micro Kit (QIAGEN). After pelleting by centrifugation for 5 minutes at 5,000 x g, the RNA protect was replaced by 350 µl buffer RLT Plus and the samples were homogenized by vortexing for 30 sec. Genomic DNA contamination was removed using gDNA Eliminator spin columns. Next, one volume of 70 % ethanol was added and the samples were applied to RNeasy MinElute spin columns followed by several wash steps. Finally, total RNA was eluted in 12 µl of nuclease free water. Purity and integrity of the RNA was assessed on the Agilent 2100 Bioanalyzer with the RNA 6000 Pico LabChip reagent set (Agilent, Palo Alto, CA, USA).

The SMARTer Ultra Low Input RNA Kit for Sequencing v4 (Clontech Laboratories, Inc., Mountain View, CA, USA) was used to generate first strand cDNA from 100 pg total-RNA. Double stranded cDNA was amplified by LD PCR (13 cycles) and purified via magnetic bead clean-up. Library preparation was carried out as described in the Illumina Nextera XT Sample Preparation Guide (Illumina, Inc., San Diego, CA, USA). 150 pg of input cDNA were tagmented (tagged and fragmented) by the Nextera XT transposome. The products were purified and amplified via a limited-cycle PCR program to generate multiplexed sequencing libraries. For the PCR step 1:5 dilutions of index 1 (i7) and index 2 (i5) primers were used. The libraries were quantified using the KAPA SYBR FAST ABI Prism Library Quantification Kit (Kapa Biosystems, Inc., Woburn, MA, USA). Equimolar amounts of each library were sequenced on a NextSeq 500 instrument controlled by the NextSeq Control Software (NCS) v2.2.0, using a 75 Cycles High Output Kit with the single index, single-read (SR) run parameters. Image analysis and base calling were done by the Real Time Analysis Software (RTA) v2.4.11. The resulting .bcl files were converted into.fastq files with the bcl2fastq v2.18 software. RNA extraction, library preparation and RNAseq were performed at the Genomics Core Facility “KFB - Center of Excellence for Fluorescent Bioanalytics” (University of Regensburg, Regensburg, Germany; www.kfb-regensburg.de). Data have been deposited in the ArrayExpress repository with the dataset identifier E-MTAB-8554.

**RNA extraction, cDNA synthesis and real-time PCR**

Cells were processed as described in previous section. RNA from TCRγδ$^{+}$CD44$^{+}$CD27$^{-}$Vγ4$^{+}$, TCRγδ$^{+}$CD44$^{+}$CD27$^{-}$Vγ4$^{-}$, TCRγδ$^{+}$CD27$^{+}$, or CD4$^{+}$ T cells was extracted using the RNeasy micro kit (Qiagen) followed by cDNA synthesis using the iScript cDNA synthesis kit (BioRad), according the manufacturers' protocol. Real-time PCR reactions were performed with SsoFast EvaGreen Supermic (BioRad) on a CFX96 (BioRad) cycler. The following primers were used: RARdn transgene Fwd-AAGCCCGAGTGCTCTGAGA, Rev-TTCGTAGTGTATTTGCCCAG; b-actin Fwd-GGCTGTATTCCCCTCCATCG, Rev-CCAGTTGGTAACAATGCCATGT.

**Data Analysis**

Flow cytometry data was analyzed using Flow Jo v9.8.3 or v10. All graphs associated to flow cytometry were generated using Prism v8 and statistically analyzed using unpaired non-parametric Mann-Whitney U-test. For EAE experiments, clinical scoring and weights were analyzed using 2-way ANOVA with Bonferroni's multiple comparisons test. The RNAseq data was initially pseudoaligned using Kallisto (*66*) with the BioMart package and the ensemble data base as reference with the Jul2019 archive. Further downstream analysis was done using the DESeq2 package for R (*67*). The DESeq2 package was also used to calculate statistical significance between sample comparisons by employing the Wald-test for p values and the Benjamini-Hochberg adjustment for padj values. Real-time data was analyzed using the Bio-Rad CFX manager software, with gene expression normalized to that of β-actin.

## References


1. M. N. Erkelens, R. E. Mebius, Retinoic Acid and Immune Homeostasis: A Balancing Act. *Trends Immunol* **38**, 168-180 (2017).
2. J. A. Hall, J. R. Grainger, S. P. Spencer, Y. Belkaid, The role of retinoic acid in tolerance and immunity. *Immunity* **35**, 13-22 (2011).
3. G. Duester, Retinoic acid synthesis and signaling during early organogenesis. *Cell* **134**, 921-931 (2008).
4. M. R. Conserva, L. Anelli, A. Zagaria, G. Specchia, F. Albano, The Pleiotropic Role of Retinoic Acid/Retinoic Acid Receptors Signaling: From Vitamin A Metabolism to Gene Rearrangements in Acute Promyelocytic Leukemia. *Int J Mol Sci* **20**, (2019).
5. N. R. de Almeida, M. Conda-Sheridan, A review of the molecular design and biological activities of RXR agonists. *Med Res Rev* **39**, 1372-1397 (2019).
6. N. B. Ghyselinck, G. Duester, Retinoic acid signaling pathways. *Development* **146**, (2019).

7. S. A. van de Pavert *et al.*, Chemokine CXCL13 is essential for lymph node initiation and is induced by retinoic acid and neuronal stimulation. *Nat Immunol* **10**, 1193-1199 (2009).
8. S. A. van de Pavert *et al.*, Maternal retinoids control type 3 innate lymphoid cells and set the offspring immunity. *Nature* **508**, 123-127 (2014).
9. W. W. Agace, E. K. Persson, How vitamin A metabolizing dendritic cells are generated in the gut mucosa. *Trends Immunol* **33**, 42-48 (2012).
10. K. M. Luda *et al.*, IRF8 Transcription-Factor-Dependent Classical Dendritic Cells Are Essential for Intestinal T Cell Homeostasis. *Immunity* **44**, 860-874 (2016).
11. M. H. Kim, E. J. Taparowsky, C. H. Kim, Retinoic Acid Differentially Regulates the Migration of Innate Lymphoid Cell Subsets to the Gut. *Immunity* **43**, 107-119 (2015).
12. J. A. Hall *et al.*, Essential role for retinoic acid in the promotion of CD4(+) T cell effector responses via retinoic acid receptor alpha. *Immunity* **34**, 435-447 (2011).
13. H. R. Cha *et al.*, Downregulation of Th17 cells in the small intestine by disruption of gut flora in the absence of retinoic acid. *J Immunol* **184**, 6799-6806 (2010).
14. J. L. Coombes *et al.*, A functionally specialized population of mucosal CD103+ DCs induces Foxp3+ regulatory T cells via a TGF-beta and retinoic acid-dependent mechanism. *J Exp Med* **204**, 1757-1764 (2007).
15. C. M. Sun *et al.*, Small intestine lamina propria dendritic cells promote de novo generation of Foxp3 T reg cells via retinoic acid. *J Exp Med* **204**, 1775-1785 (2007).
16. D. Mucida *et al.*, Reciprocal TH17 and regulatory T cell differentiation mediated by retinoic acid. *Science* **317**, 256-260 (2007).
17. C. C. Brown *et al.*, Retinoic acid is essential for Th1 cell lineage stability and prevents transition to a Th17 cell program. *Immunity* **42**, 499-511 (2015).
18. B. S. Reis, D. P. Hoytema van Konijnenburg, S. I. Grivennikov, D. Mucida, Transcription factor T-bet regulates intraepithelial lymphocyte functional maturation. *Immunity* **41**, 244-256 (2014).
19. B. S. Reis, A. Rogoz, F. A. Costa-Pinto, I. Taniuchi, D. Mucida, Mutual expression of the transcription factors Runx3 and ThPOK regulates intestinal CD4(+) T cell immunity. *Nat Immunol* **14**, 271-280 (2013).
20. D. Kadekar *et al.*, The neonatal microenvironment programs innate gammadelta T cells through the transcription factor STAT5. *J Clin Invest* **130**, 2496-2508 (2020).
21. C. E. Sutton *et al.*, Interleukin-1 and IL-23 induce innate IL-17 production from gammadelta T cells, amplifying Th17 responses and autoimmunity. *Immunity* **31**, 331-341 (2009).
22. Ivanov, II *et al.*, The orphan nuclear receptor RORgammat directs the differentiation program of proinflammatory IL-17+ T helper cells. *Cell* **126**, 1121-1133 (2006).
23. C. A. Dendrou, L. Fugger, M. A. Friese, Immunopathology of multiple sclerosis. *Nat Rev Immunol* **15**, 545-558 (2015).
24. M. Hiltensperger, T. Korn, The Interleukin (IL)-23/T helper (Th)17 Axis in Experimental Autoimmune Encephalomyelitis and Multiple Sclerosis. *Cold Spring Harb Perspect Med* **8**, (2018).
25. L. Schirmer, V. Rothhammer, B. Hemmer, T. Korn, Enriched CD161high CCR6+ gammadelta T cells in the cerebrospinal fluid of patients with multiple sclerosis. *JAMA Neurol* **70**, 345-351 (2013).
26. J. van Langelaar *et al.*, T helper 17.1 cells associate with multiple sclerosis disease activity: perspectives for early intervention. *Brain* **141**, 1334-1349 (2018).
27. E. Havrdova *et al.*, Activity of secukinumab, an anti-IL-17A antibody, on brain lesions in RRMS: results from a randomized, proof-of-concept study. *J Neurol* **263**, 1287-1295 (2016).

28. C. Luckel *et al.*, IL-17(+) CD8(+) T cell suppression by dimethyl fumarate associates with clinical response in multiple sclerosis. *Nature communications* **10**, 5722 (2019).
29. V. Cipollini, J. Anrather, F. Orzi, C. Iadecola, Th17 and Cognitive Impairment: Possible Mechanisms of Action. *Front Neuroanat* **13**, 95 (2019).
30. C. Klemann *et al.*, Synthetic retinoid AM80 inhibits Th17 cells and ameliorates experimental autoimmune encephalomyelitis. *Am J Pathol* **174**, 2234-2245 (2009).
31. M. Raverdeau, C. J. Breen, A. Misiak, K. H. Mills, Retinoic acid suppresses IL-17 production and pathogenic activity of gammadelta T cells in CNS autoimmunity. *Immunol Cell Biol* **94**, 763-773 (2016).
32. J. Xu, P. D. Drew, 9-Cis-retinoic acid suppresses inflammatory responses of microglia and astrocytes. *J Neuroimmunol* **171**, 135-144 (2006).
33. M. R. Mizee *et al.*, Astrocyte-derived retinoic acid: a novel regulator of blood-brain barrier function in multiple sclerosis. *Acta Neuropathol* **128**, 691-703 (2014).
34. C. Tryfonos *et al.*, Dietary Supplements on Controlling Multiple Sclerosis Symptoms and Relapses: Current Clinical Evidence and Future Perspectives. *Medicines (Basel)* **6**, (2019).
35. M. Lochner *et al.*, In vivo equilibrium of proinflammatory IL-17+ and regulatory IL-10+ Foxp3+ RORgamma t+ T cells. *J Exp Med* **205**, 1381-1393 (2008).
36. F. Rajaii, Z. T. Bitzer, Q. Xu, S. Sockanathan, Expression of the dominant negative retinoid receptor, RAR403, alters telencephalic progenitor proliferation, survival, and cell fate specification. *Dev Biol* **316**, 371-382 (2008).
37. J. D. Haas *et al.*, CCR6 and NK1.1 distinguish between IL-17A and IFN-gamma-producing gammadelta effector T cells. *Eur J Immunol* **39**, 3488-3497 (2009).
38. J. C. Ribot *et al.*, CD27 is a thymic determinant of the balance between interferon-gamma- and interleukin 17-producing gammadelta T cell subsets. *Nat Immunol* **10**, 427-436 (2009).
39. J. S. Heilig, S. Tonegawa, Diversity of murine gamma genes and expression in fetal and adult T lymphocytes. *Nature* **322**, 836-840 (1986).
40. A. M. McGinley *et al.*, Interleukin-17A Serves a Priming Role in Autoimmunity by Recruiting IL-1beta-Producing Myeloid Cells that Promote Pathogenic T Cells. *Immunity* **52**, 342-356 e346 (2020).
41. R. Agerholm, J. Rizk, M. T. Vinals, V. Bekiaris, STAT3 but not STAT4 is critical for gammadeltaT17 cell responses and skin inflammation. *EMBO Rep*, e48647 (2019).
42. E. E. Gray *et al.*, Deficiency in IL-17-committed Vgamma4(+) gammadelta T cells in a spontaneous Sox13-mutant CD45.1(+) congenic mouse substrain provides protection from dermatitis. *Nat Immunol* **14**, 584-592 (2013).
43. V. Bekiaris, J. R. Sedy, M. G. Macauley, A. Rhode-Kurnow, C. F. Ware, The Inhibitory Receptor BTLA Controls gammadelta T Cell Homeostasis and Inflammatory Responses. *Immunity* **39**, 1082-1094 (2013).
44. M. L. Michel *et al.*, Interleukin 7 (IL-7) selectively promotes mouse and human IL-17-producing gammadelta cells. *Proc Natl Acad Sci U S A* **109**, 17549-17554 (2012).
45. K. Shibata *et al.*, Notch-Hes1 pathway is required for the development of IL-17-producing gammadelta T cells. *Blood* **118**, 586-593 (2011).
46. R. Baccala *et al.*, Gamma delta T cell homeostasis is controlled by IL-7 and IL-15 together with subset-specific factors. *J Immunol* **174**, 4606-4612 (2005).
47. E. Eden, R. Navon, I. Steinfeld, D. Lipson, Z. Yakhini, GOrilla: a tool for discovery and visualization of enriched GO terms in ranked gene lists. *BMC Bioinformatics* **10**, 48 (2009).
48. E. Eden, D. Lipson, S. Yogev, Z. Yakhini, Discovering motifs in ranked lists of DNA sequences. *PLoS Comput Biol* **3**, e39 (2007).

49. S. P. Singh, H. H. Zhang, J. F. Foley, M. N. Hedrick, J. M. Farber, Human T cells that are able to produce IL-17 express the chemokine receptor CCR6. *J Immunol* **180**, 214-221 (2008).
50. J. Chen *et al.*, The RNA-binding protein HuR contributes to neuroinflammation by promoting C-C chemokine receptor 6 (CCR6) expression on Th17 cells. *J Biol Chem* **292**, 14532-14543 (2017).
51. A. Reboldi *et al.*, C-C chemokine receptor 6-regulated entry of TH-17 cells into the CNS through the choroid plexus is required for the initiation of EAE. *Nat Immunol* **10**, 514-523 (2009).
52. B. E. Theien *et al.*, Discordant effects of anti-VLA-4 treatment before and after onset of relapsing experimental autoimmune encephalomyelitis. *J Clin Invest* **107**, 995-1006 (2001).
53. K. G. Haanstra *et al.*, Antagonizing the alpha4beta1 integrin, but not alpha4beta7, inhibits leukocytic infiltration of the central nervous system in rhesus monkey experimental autoimmune encephalomyelitis. *J Immunol* **190**, 1961-1973 (2013).
54. G. P. Rice, H. P. Hartung, P. A. Calabresi, Anti-alpha4 integrin therapy for multiple sclerosis: mechanisms and rationale. *Neurology* **64**, 1336-1342 (2005).
55. J. Ransom, P. J. Morgan, P. J. McCaffery, P. N. Stoney, The rhythm of retinoids in the brain. *J Neurochem* **129**, 366-376 (2014).
56. N. Noy, Between death and survival: retinoic acid in regulation of apoptosis. *Annu Rev Nutr* **30**, 201-217 (2010).
57. S. G. Kang, J. Park, J. Y. Cho, B. Ulrich, C. H. Kim, Complementary roles of retinoic acid and TGF-beta1 in coordinated expression of mucosal integrins by T cells. *Mucosal Immunol* **4**, 66-82 (2011).
58. M. Iwata *et al.*, Retinoic acid imprints gut-homing specificity on T cells. *Immunity* **21**, 527-538 (2004).
59. L. Tan *et al.*, Single-Cell Transcriptomics Identifies the Adaptation of Scart1(+) Vgamma6(+) T Cells to Skin Residency as Activated Effector Cells. *Cell reports* **27**, 3657-3671 e3654 (2019).
60. T. Chen *et al.*, Epicardial induction of fetal cardiomyocyte proliferation via a retinoic acid-inducible trophic factor. *Dev Biol* **250**, 198-207 (2002).
61. L. Lai, B. L. Bohnsack, K. Niederreither, K. K. Hirschi, Retinoic acid regulates endothelial cell proliferation during vasculogenesis. *Development* **130**, 6465-6474 (2003).
62. D. F. Nino *et al.*, Retinoic Acid Improves Incidence and Severity of Necrotizing Enterocolitis by Lymphocyte Balance Restitution and Repopulation of LGR5+ Intestinal Stem Cells. *Shock* **47**, 22-32 (2017).
63. A. Ertesvag, N. Engedal, S. Naderi, H. K. Blomhoff, Retinoic acid stimulates the cell cycle machinery in normal T cells: involvement of retinoic acid receptor-mediated IL-2 secretion. *J Immunol* **169**, 5555-5563 (2002).
64. N. Engedal, T. Gjevik, R. Blomhoff, H. K. Blomhoff, All-trans retinoic acid stimulates IL-2-mediated proliferation of human T lymphocytes: early induction of cyclin D3. *J Immunol* **177**, 2851-2861 (2006).
65. G. Eberl, D. R. Littman, Thymic origin of intestinal alphabeta T cells revealed by fate mapping of RORgammat+ cells. *Science* **305**, 248-251 (2004).
66. N. L. Bray, H. Pimentel, P. Melsted, L. Pachter, Near-optimal probabilistic RNA-seq quantification. *Nat Biotechnol* **34**, 525-527 (2016).
67. M. I. Love, W. Huber, S. Anders, Moderated estimation of fold change and dispersion for RNA-seq data with DESeq2. *Genome Biol* **15**, 550 (2014).

## Acknowledgments

We are grateful to Professors William Agace (Lund University, Sweden, and DTU, Denmark) and Shan Sockanathan (Johns Hopkins School of Medicine, MD) for providing us with RARdn$^{F/F}$ mice and Professor Gerard Eberl (Pasteur, Paris, France) for providing us with RORγt$^{CRE}$ mice. The study and VB were supported by the Lundbeck Foundation (R163-2013-15201), RA and JR were supported by DTU PhD scholarships, DK was supported by the Leo Foundation (LF16020), AB was supported by Novo Nordisk Foundation (NNF1OC0052931), and SRH supported by Lundbeck Foundation (R190-2014-4178)

# Figures

## Figure 1

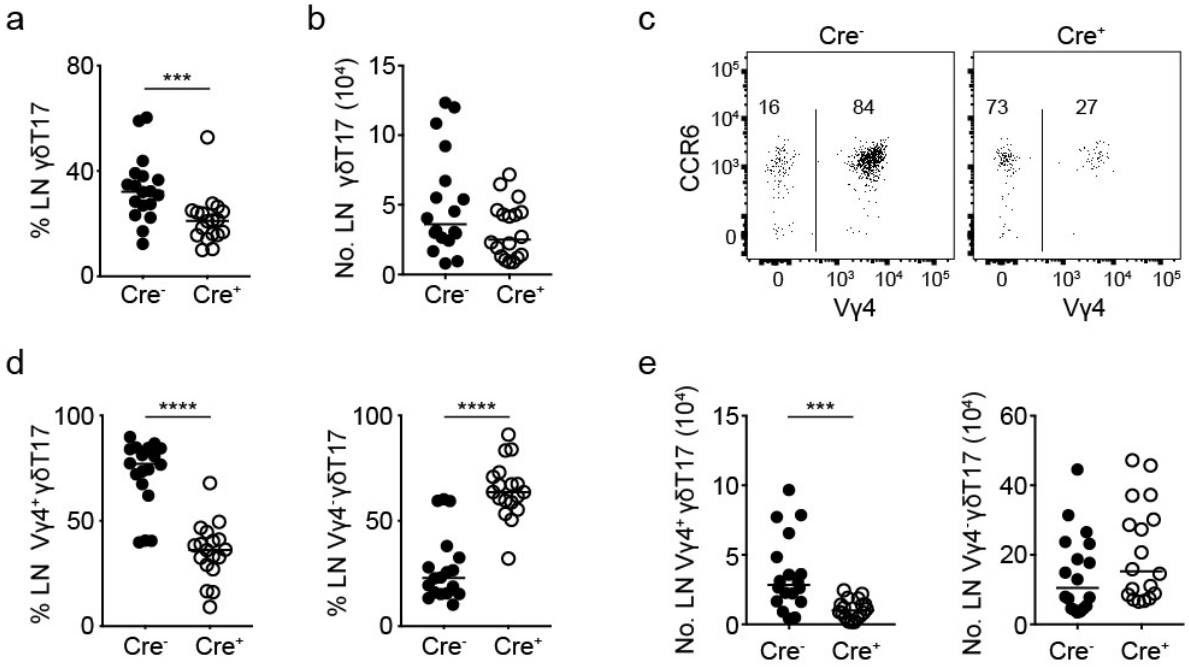


**Fig1. Aberrant homeostasis of γδT17 cell populations in the lymph node of RORγt$^{CRE}$-RARdn$^{F/F}$ mice.**

Flow cytometric analysis of γδ T cells in RORγt$^{CRE}$-RARdn$^{F/F}$ (Cre$^{+}$) and littermate control mice (Cre$^{-}$). In graphs, each symbol represents a mouse and line the median. ***p < 0.001, ****p < 0.0001 using Mann-Whitney test. (**A, B**) Frequency (**A**) and numbers (**B**) of γδT17 (CD27$^{-}$CD44$^{+}$TCRγδ$^{+}$TCRβ$^{-}$) cells in the LN. (**C**) Expression of Vγ4 and CCR6 within the γδT17 compartment; numbers indicate frequency of Vγ4$^{+}$ and Vγ4$^{-}$ cells. (**D**) Frequency of Vγ4$^{+}$ (left) and Vγ4$^{-}$ (right) γδT17 cells in the LN. (**E**) Numbers of Vγ4$^{+}$ (left) and Vγ4$^{-}$ (right) γδT17 cells in the LN. *n* = 5 experiments, 18 mice per genotype.

Figure 2

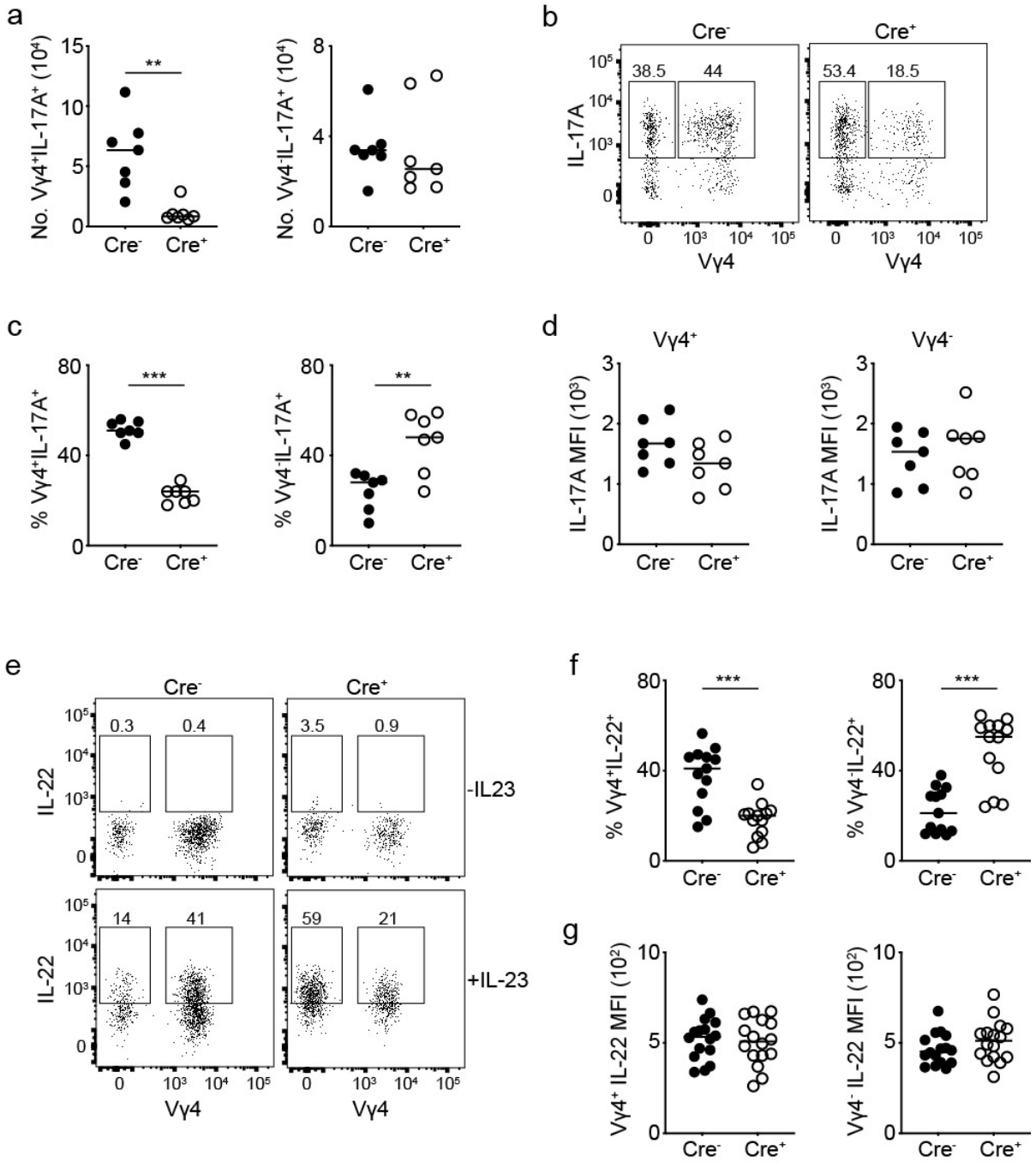


**Figure 2. Production of IL-17A and IL-22 by γδT17 cells in independent of RAR.**

Flow cytometric analysis of cytokine-producing γδ T cells in RORγt$^{CRE}$-RARdn$^{F/F}$ (Cre$^{+}$) and littermate control mice (Cre$^{-}$). In graphs, each symbol represents a mouse and line the median. **p < 0.01, ***p < 0.001 using Mann-Whitney test. (**A**) Numbers of Vγ4$^{+}$IL-17A$^{+}$ (left) and Vγ4$^{-}$IL-17A$^{+}$ (right) γδT17 cells. (**B**) Expression of Vγ4 and IL-17A within the γδT17 compartment; numbers indicate frequencies of Vγ4$^{+}$IL-17A$^{+}$ and Vγ4$^{-}$IL-17A$^{+}$ cells. (**C**) Frequency of Vγ4$^{+}$IL-17A$^{+}$ (left) and

618 Vγ4$^{-}$IL-17A$^{+}$ (right) γδT17 cells. (**D**) Mean fluorescent intensity (MFI) of IL-17A staining in Vγ4$^{+}$
619 (left) and Vγ4$^{-}$ (right) γδT17 cells. (**E**) Expression of Vγ4 and IL-22 within the γδT17 compartment
620 in the presence or absence of IL-23 stimulation; numbers indicate frequency of Vγ4$^{+}$IL-22$^{+}$ and
621 Vγ4$^{-}$IL-22$^{+}$ cells. (**F**) Frequency of Vγ4$^{+}$IL-22$^{+}$ (left) and Vγ4$^{-}$IL-22$^{+}$ (right) γδT17 cells after IL-23
622 stimulation. (**G**) MFI of IL-22 staining in Vγ4$^{+}$ (left) and Vγ4$^{-}$ (right) γδT17 cells after IL-23
623 stimulation. *n* = 3 experiments, 7 mice per genotype (a-d); or *n* = 5 experiments, 13 mice per
624 genotype (e, f, g).

Figure 3

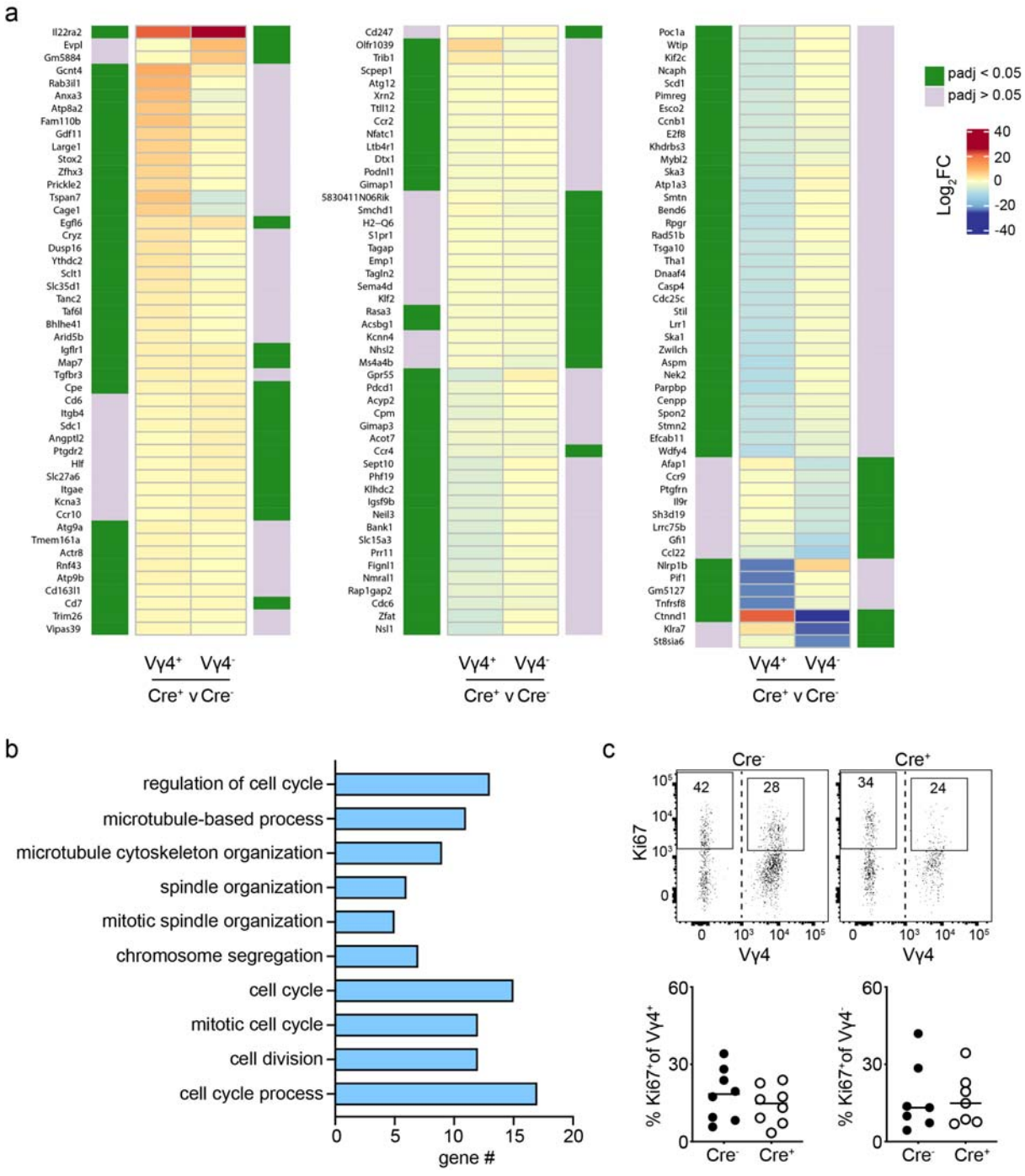


**Figure 3. Regulation of cell cycle genes by RAR in γδT17 cell populations.**

Analysis of differentially expressed genes in Vγ4$^+$ and Vγ4$^-$ γδT17 cells isolated from RORγt$^{CRE}$-RARdn$^{F/F}$ (Cre$^+$) or littermate control mice (Cre$^-$) after RNA-sequencing. Data is representative of 3 biological repeats. (**A**) Heatmap showing the average $Log_2FC$ (fold-change) of significantly changed genes in either Vγ4$^+$ or Vγ4$^-$ cells. Genes with significant $Log_2FC$ (padj < 0.05) in each comparison are marked as green in the adjacent column, while insignificant changes (padj > 0.05)

are marked as purple. (**B**) GOrilla pathway analysis of the differentially downregulated genes (padj < 0.05) in Vγ4$^{+}$ cells from RORγt$^{CRE}$-RARdn$^{F/F}$ (Cre$^{+}$) compared to littermate control mice (Cre$^{-}$). Number of enriched genes in each pathway is shown on the x-axis and the pathways are arranged by significance score on the y-axis (only significantly enriched pathways are shown). (**C**) Flow cytometric analysis of Ki67 expression in γδT17 cells in RORγt$^{CRE}$-RARdn$^{F/F}$ (Cre$^{+}$) and littermate control mice (Cre$^{-}$); numbers in FACS plots indicate frequencies of Ki67$^{+}$ cells within the Vγ4$^{+}$ or Vγ4$^{-}$ compartments; in graphs, each symbol represents a mouse and line the median; *n* = 4 experiments, 7-8 mice per genotype.

Figure 4

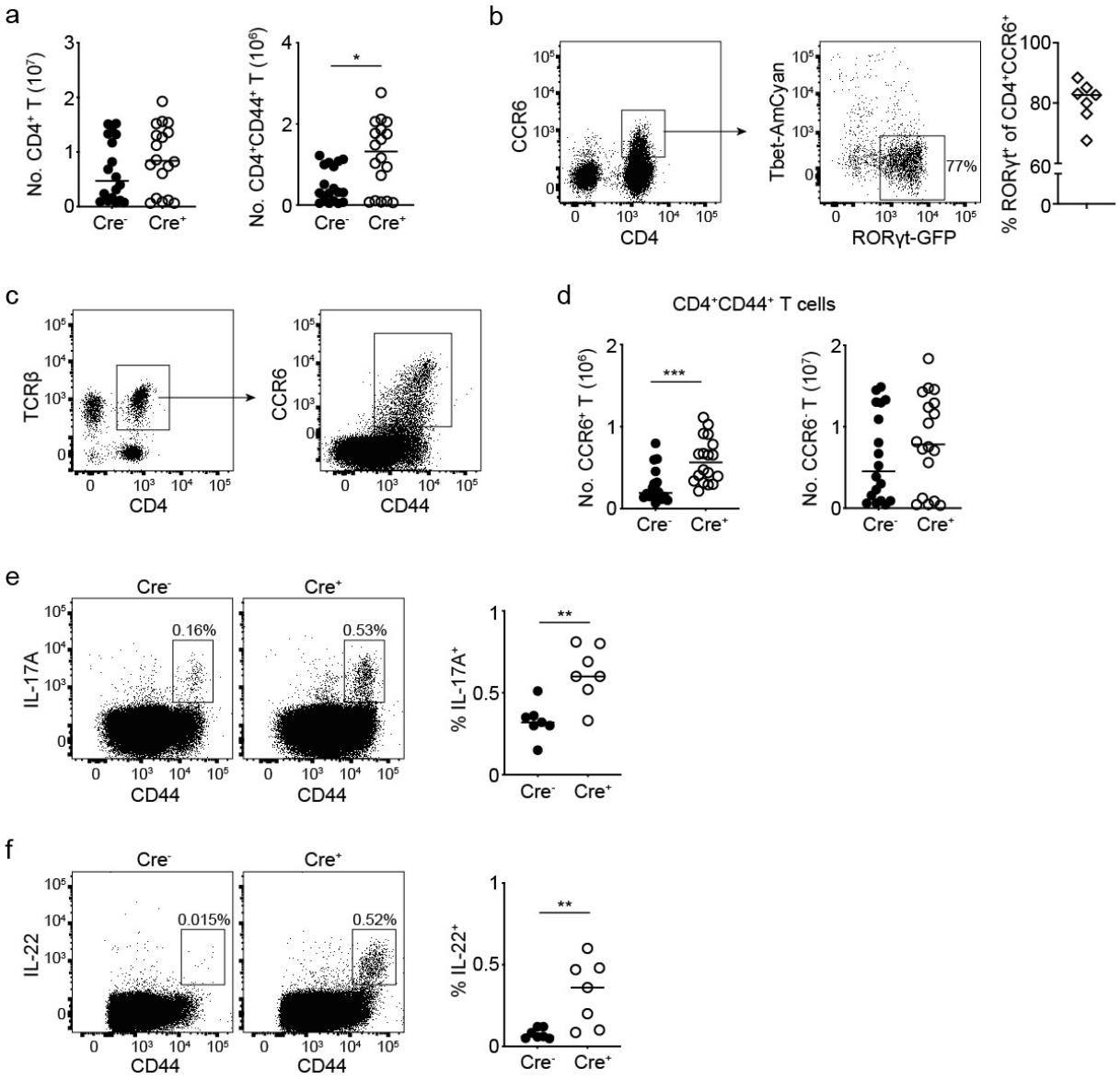


**Figure 4. RAR negatively regulates the homeostasis of $T_H17$ cells.**

642 Flow cytometric analysis of lymph node $CD4^+$ T cells in $ROR\gamma t^{CRE}$-$RARdn^{F/F}$ ($Cre^+$) and littermate
643 control mice ($Cre^-$) unless specified. In graphs, each symbol represents a mouse and line the
644 median. *$p < 0.05$, **$p < 0.01$, ***$p < 0.001$ using Mann-Whitney test. (**A**) Numbers of $CD4^+$ (left)
645 and $CD4^+CD44^+$ (right) T cells. (**B**) Expression of CD4 and CCR6 within the TCRβ compartment
646 (left) of $ROR\gamma t^{GFP}$-$Tbet^{AmCyan}$ mice, and frequency of RORγt-$GFP^+$ cells within the $CD4^+CCR6^+$ gate
647 (right). (**C**) Expression of CD4 and TCRβ within the lymphocyte compartment (left), and expression
648 of CD44 and CCR6 within the $CD4^+TCR\beta^+$ gate (right). (**D**) Numbers of $CCR6^+$ (left) and $CCR6^-$
649 (right) cells within the $CD4^+CD44^+$ compartment. (**E**) Expression of CD44 and IL-17A, and
650 frequency of IL-$17A^+$ cells within the $CD4^+TCR\beta^+$ compartment; numbers in FACS plots indicate
651 frequencies of IL-$17A^+$ cells. (**F**) Expression of CD44 and IL-22, and frequency of IL-$22^+$ cells within
652 the $CD4^+TCR\beta^+$ compartment; numbers in FACS plots indicate frequencies of IL-$22^+$ cells. *n* = 5
653 experiments, 18 mice per genotype (a, c, d); *n* = 1 experiment, 7 mice (b); or *n* = 3 experiments, 7
654 mice per genotype (e, f).

Figure 5

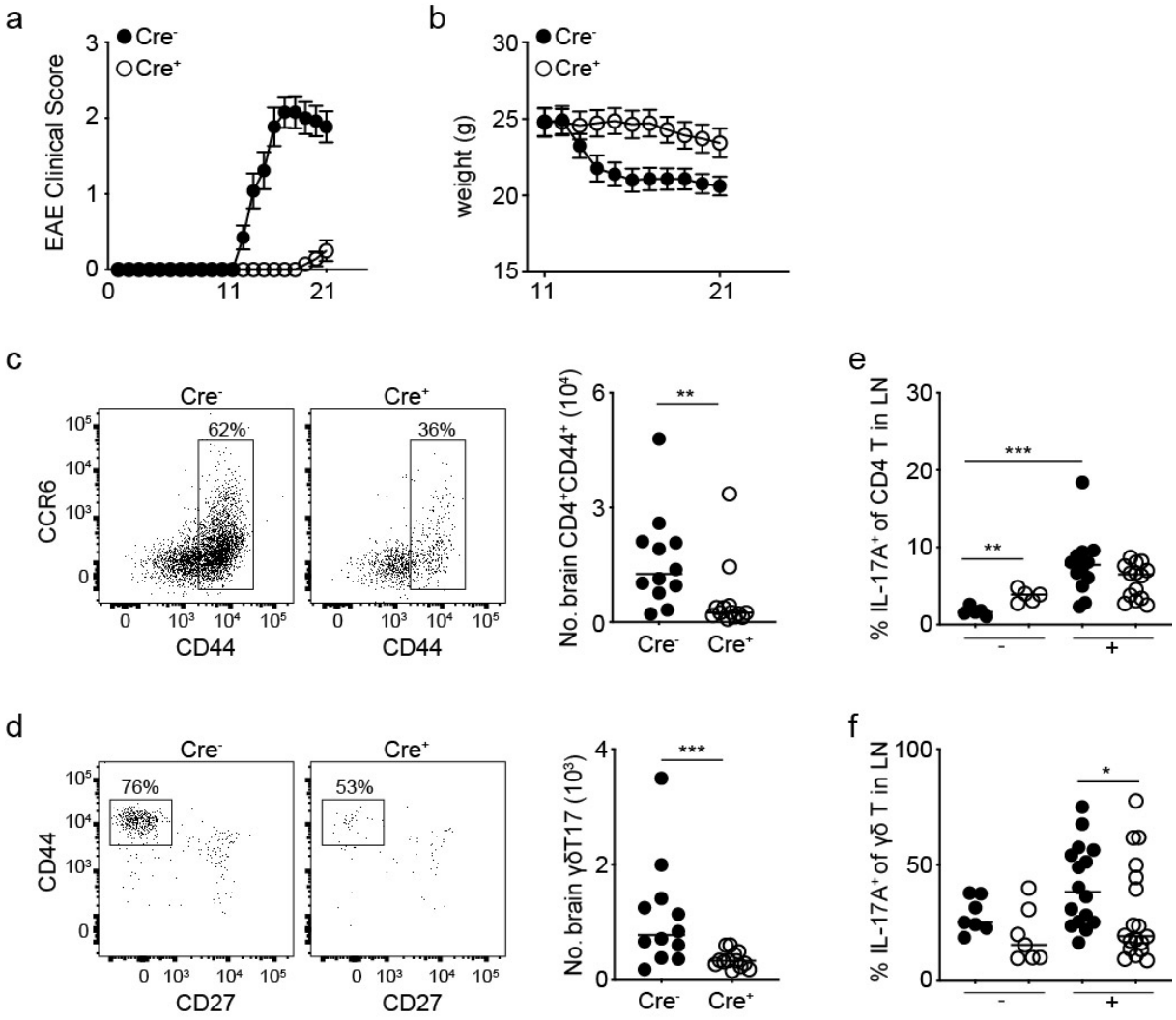


**Figure 5. RAR is necessary for EAE pathogenesis.**

Disease progression and flow cytometric analysis of γδ and $CD4^+$ T cells in $ROR\gamma t^{CRE}$-$RARdn^{F/F}$ ($Cre^+$) and littermate control mice ($Cre^-$) before (−) and 21 days after (+) EAE induction. In graphs, each symbol represents a mouse and line the median (except in **A**, **B**). *p < 0.05, **p < 0.01, ***p < 0.001 using Mann-Whitney test. (**A**, **B**) Clinical symptoms of EAE (**A**) and mouse weight (**B**); data is a pool of 13-14 mice per genotype from 4 experiments and shown as mean±sem; 2-way ANOVA with Bonferroni's multiple comparisons test returned significance for days 14-21 p < 0.0001 (**A**) and days 15-17 p < 0.05 (**B**). (**C**) Expression of CD44 and CCR6 in the $CD4^+TCR\beta^+$ compartment, and numbers of $CD4^+CD44^+$ T cells in the brain; numbers in FACS plots indicate $CD44^+$ cell frequencies. (**D**) Expression of CD27 and CD44 in the $TCR\gamma\delta^+TCR\beta^-$ compartment, and numbers

of γδT17 ($CD27^{-}CD44^{+}$) T cells in the brain; numbers in FACS plots indicate γδT17 cell frequencies. (**E**) Frequency of IL-$17A^{+}$ cells within the LN $CD4^{+}TCR\beta^{+}$ compartment. (**F**) Frequency of IL-$17A^{+}$ cells within the LN $TCR\gamma\delta^{+}TCR\beta^{-}$ compartment. *n* = 4 experiments, 7 control or 16-18 EAE mice per genotype.

Figure 6

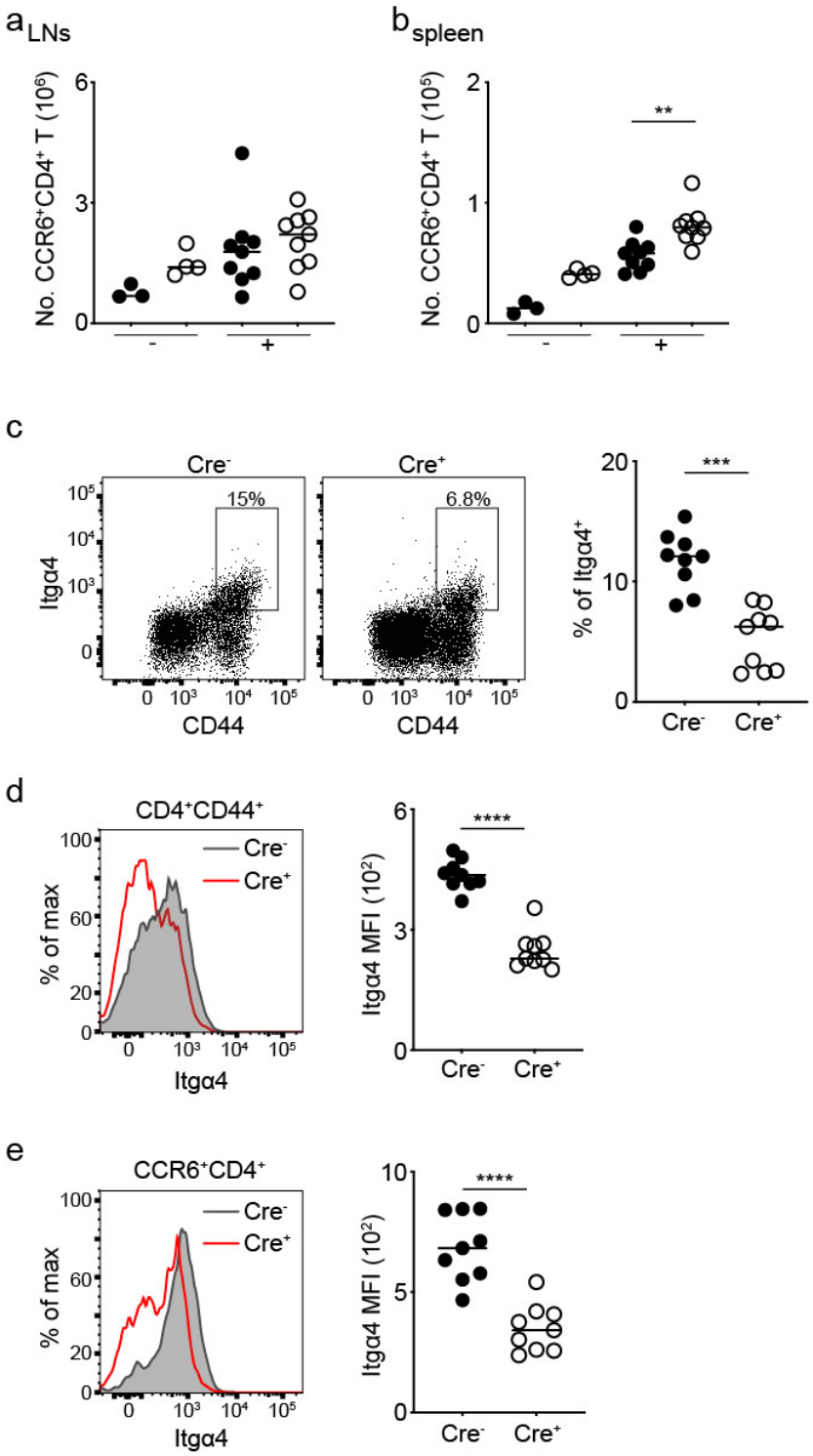


**Figure 6. RAR regulates integrin-α4 on CD4$^+$ T cells but not their expansion during the early phase of EAE.**

Flow cytometric analysis of lymph node (a) and splenic (b-e) CD4$^+$ T cells in RORγt$^{CRE}$-RARdn$^{F/F}$ (Cre$^+$) and littermate control mice (Cre$^-$) before (−) and 11 days after (+) EAE induction. In graphs,

each symbol represents a mouse and line the median. **p < 0.01, ***p < 0.001, ****p < 0.0001 using Mann-Whitney test. (**A**, **B**) Numbers of $CCR6^+CD4^+$ T cells in the LNs (**A**) and spleen (**B**) before (−) and 11 days after (+) EAE induction. (**C**) Expression of CD44 and Itgα4, and frequency of $Itgα4^+$ cells within the $CD4^+TCRβ^+$ compartment at day 11; numbers in FACS plots indicate frequencies of $Itgα4^+$ cells. (**D**, **E**) Expression of Itgα4, and MFI of Itgα4 staining in $CD4^+CD44^+$ (**D**) and in $CCR6^+CD4^+$ (**E**) T cells at day 11. *n* = 3 experiments, 5-6 control or 13 EAE mice per genotype (a, b); or *n* = 2 experiments, 9 mice per genotype (c-e).

# Figure 7

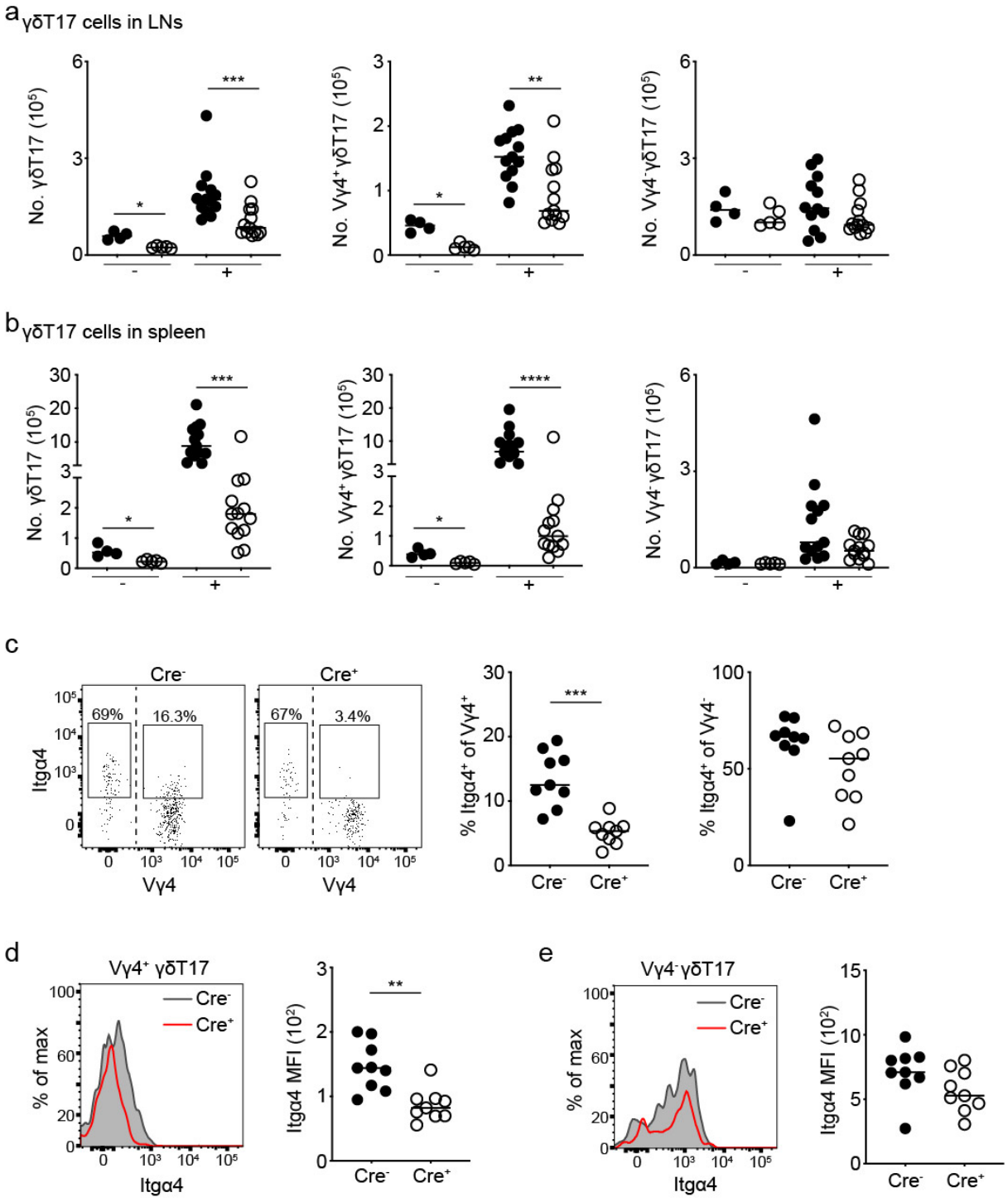


**Figure 7. RAR is necessary for optimal expansion of γδT17 cells and the expression of integrin-α4 during the early phase of EAE.**

Flow cytometric analysis of lymph node (**A**) and splenic (**B**-**E**) γδT17 cells in RORγt$^{CRE}$-RARdn$^{F/F}$ (Cre$^{+}$) and littermate control mice (Cre$^{-}$) before (−) and 11 days after (+) EAE induction. In graphs,

each symbol represents a mouse and line the median. *p < 0.05, **p < 0.01, ***p < 0.001, ****p < 0.0001 using Mann-Whitney test. (**A**, **B**) Numbers of total γδT17 (left), Vγ4$^+$ (middle) and Vγ4$^-$ (right) cells in LNs (**A**) and spleen (**B**) before (−) and 11 days after (+) EAE induction. (**C**) Expression of Vγ4 and Itgα4 within the γδT17 compartment, and frequency of Itgα4$^+$ cells within the Vγ4$^+$ or Vγ4$^-$ compartments at day 11; numbers in FACS plots indicate frequencies of Itgα4$^+$ cells within Vγ4$^+$ or Vγ4$^-$ compartments. (**D**, **E**) Expression of Itgα4, and MFI of Itgα4 staining in Vγ4$^+$ (**E**) and in Vγ4$^-$ (**E**) γδT17 cells at day 11. *n* = 3 experiments, 5-6 control or 13 EAE mice per genotype (a, b); or *n* = 2 experiments, 9 mice per genotype (c-e).